Identification of cell cycle–arrested quiescent osteoclast precursors in vivo

Toshihide Mizoguchi,[1] Akinori Muto,[1,4] Nobuyuki Udagawa,[2] Atsushi Arai,[1] Teruhito Yamashita,[1] Akihiro Hosoya,[3] Tadashi Ninomiya,[1] Hiroaki Nakamura,[3] Yohei Yamamoto,[1] Saya Kinugawa,[1] Midori Nakamura,[2] Yuko Nakamichi,[1] Yasuhiro Kobayashi,[1] Sakae Nagasawa,[1] Kimimitsu Oda,[5] Hirofumi Tanaka,[6] Mitsuo Tagaya,[6] Josef M. Penninger,[7] Michio Ito,[1] and Naoyuki Takahashi[1]

[1]Institute for Oral Science, [2]Department of Biochemistry, and [3]Department of Oral Histology, Matsumoto Dental University, Nagano 399-0781, Japan
[4]Department of Periodontology, School of Dentistry, Aichi Gakuin University, Aichi 464-8651, Japan
[5]Department of Biochemistry, School of Dentistry, Niigata University, Niigata 951-8514, Japan
[6]School of Life Science, Tokyo University of Pharmacy and Life Science, Tokyo 192-0392, Japan
[7]Institute of Molecular Biotechnology of the Austrian Academy of Sciences, A-1030 Vienna, Austria

Osteoclasts are multinucleated cells that resorb bone. Although osteoclasts originate from the monocyte/macrophage lineage, osteoclast precursors are not well characterized in vivo. The relationship between proliferation and differentiation of osteoclast precursors is examined in this study using murine macrophage cultures treated with macrophage colony-stimulating factor (M-CSF) and receptor activator of NF-κB (RANK) ligand (RANKL). Cell cycle–arrested quiescent osteoclast precursors (QuOPs) were identified as the committed osteoclast precursors in vitro. In vivo experiments show that QuOPs survive for several weeks and differentiate into osteoclasts in response to M-CSF and RANKL. Administration of 5-fluorouracil to mice induces myelosuppression, but QuOPs survive and differentiate into osteoclasts in response to an active vitamin D_3 analogue given to those mice. Mononuclear cells expressing c-Fms and RANK but not Ki67 are detected along bone surfaces in the vicinity of osteoblasts in RANKL-deficient mice. These results suggest that QuOPs preexist at the site of osteoclastogenesis and that osteoblasts are important for maintenance of QuOPs.

Introduction

Osteoclasts are multinucleated cells responsible for bone resorption (Martin et al., 1998; Roodman, 1999; Chambers, 2000). Hemopoietic cells of the monocyte/macrophage lineage differentiate into osteoclasts under the strict control of bone-forming osteoblasts (Suda et al., 1999; Takahashi et al., 2002). Osteoblasts express two cytokines essential for osteoclast differentiation, macrophage colony-stimulating factor (M-CSF) and receptor activator of NF-κB (RANK) ligand (RANKL; Suda et al., 1999; Arron and Choi, 2000; Hofbauer et al., 2000; Takahashi et al., 2002; Boyle et al., 2003). M-CSF is constitutively produced by osteoblasts. Osteopetrotic op/op mice cannot produce functionally active M-CSF as a result of an extra thymidine in the coding region of the M-CSF gene. Osteoclast formation is severely suppressed in op/op mice (Felix et al., 1990; Wiktor-Jedrzejczak et al., 1990; Yoshida et al., 1990; Kodama et al., 1991). However, RANKL is inducibly expressed as a membrane-associated factor by osteoblasts in response to osteotropic hormones such as parathyroid hormone (PTH) and 1α,25-dihydroxyvitamin D_3 ($1\alpha,25(OH)_2D_3$; Suda et al., 1999). RANKL-deficient ($RANKL^{-/-}$) mice also exhibit severe osteopetrosis because of a lack of osteoclasts (Kong et al., 1999; Suda et al., 1999; Arron and Choi, 2000; Hofbauer et al., 2000; Takahashi et al., 2002; Boyle et al., 2003). Osteoclast precursors such as bone marrow–derived macrophages (BMMΦ) express c-Fms (M-CSF receptors) and RANK (RANKL receptors), recognize RANKL expressed by osteoblasts through cell–cell interaction, and differentiate into osteoclasts in the presence of M-CSF. Although the mechanisms by which the monocyte/macrophage lineage cells differentiate into osteoclasts are

Correspondence to Naoyuki Takahashi: takahashinao@po.mdu.ac.jp

Abbreviations used in this paper: ALP, alkaline phosphatase; HSC, hematopoietic stem cell; HU, hydroxyurea; LPS, lipopolysaccharide; M-CSF, macrophage colony-stimulating factor; PTH, parathyroid hormone; QuOP, quiescent osteoclast precursor; RANK, receptor activator of NF-κB; RANKL, RANK ligand; TRAP, tartrate-resistant acid phosphatase.

The Rockefeller University Press $30.00
J. Cell Biol. Vol. 184 No. 4 541–554
www.jcb.org/cgi/doi/10.1083/jcb.200806139

well defined, the characteristics of the osteoclast precursors in vivo have remained unclear.

Using RANKL$^{-/-}$ mice and a system involving bone morphogenetic protein 2 (BMP-2)–induced ectopic bone formation, we previously examined how the site of osteoclastogenesis is determined (Yamamoto et al., 2006). Collagen disks containing BMP-2 (BMP-2 disks) or vehicle were implanted into RANKL$^{-/-}$ mice, which were i.p. injected with RANKL for 7 d. Tartrate-resistant acid phosphatase (TRAP; a marker enzyme of osteoclasts)–positive (TRAP^{+}) osteoclasts and alkaline phosphatase (ALP; a marker enzyme of osteoblasts)–positive (ALP^{+}) osteoblasts simultaneously appeared in the BMP-2 disks but not in the control disks. TRAP^{+} osteoclasts were located in close proximity to ALP^{+} osteoblasts. These results suggest that osteoblasts also play important roles in osteoclastogenesis by providing a suitable microenvironment for the action of RANKL. Recent studies have established that immunoreceptor tyrosine-based activation motif–mediated signals act as a costimulatory signal in RANKL-induced osteoclastogenesis (Kim et al., 2002; Koga et al., 2004). Osteoblasts are proposed to express the putative ligand for immunoglobulin-like receptors, which induces signals mediated by immunoreceptor tyrosine-based activation motif–containing molecules. These results suggest that, besides M-CSF and RANKL, unknown osteoblast-derived factors and ligands for immunoglobulin-like receptors may be involved in the determination of the correct location of osteoclast formation.

Hematopoietic stem cells (HSCs) have self-renewal capacity and multilineage developmental potentials (Wilson and Trumpp, 2006). A specific microenvironment in bone, called a stem cell niche, is proposed to sustain HSCs in an immature state so that their numbers can be maintained without a loss of properties. HSCs that exist in the niche are shown to be resistant to treatment with 5-fluorouracil (5-FU), which induces apoptosis in proliferating cells (Heissig et al., 2002; Arai et al., 2004). Recent studies have shown that HSCs are located in the trabecular endosteum area where osteoblasts play a critical role in maintaining quiescent HSCs (Zhang et al., 2003; Arai et al., 2004). It was also shown that PTH, through activation of the PTH/PTH-related peptide receptor in osteoblasts, could alter the HSC niche, resulting in the expansion of HSCs in vivo and in vitro (Calvi et al., 2003). These results suggest that osteoblasts also play a role in the regulation of hematopoiesis.

Cell proliferation and differentiation are coordinated processes in the development of specialized cells. Cell proliferation is driven by heterodimeric kinases composed of a cyclin, a regulatory subunit, and a Cdk, a catalytic subunit (Morgan, 1995; Sherr and Roberts, 1999). However, Cdk inhibitors such as the Cip/Kip family (p21^{CIP1}, p27^{KIP1}, and p57^{KIP2}) regulate the activity of Cdks (Sherr and Roberts, 1995, 1999; Sherr, 1996; Nakayama, 1998; Pavletich, 1999). Both cell cycle progression and withdrawal are tightly controlled by these cell cycle regulatory molecules. Recent studies have shown that p27^{KIP1}- and p21^{CIP1}-induced cell cycle withdrawal in osteoclast precursors is important for their differentiation into osteoclasts (Okahashi et al., 2001; Sankar et al., 2004).

In this study, we examined the relationship between proliferation and differentiation of osteoclast precursors in murine BMMΦ cultures and identified cell cycle–arrested quiescent osteoclast precursors (QuOPs) as the committed osteoclast precursors. In vivo experiments showed that QuOPs detected in bone had a long lifespan and promptly differentiated into osteoclasts in response to bone resorption-inducing stimuli. Like HSCs, QuOPs showed marked resistance to 5-FU treatment and preexisted along bone surfaces in the close vicinity of osteoblasts. Our results provide the first description of cell cycle–arrested osteoclast precursors in vivo.

Results

Cell cycle arrest in osteoclast precursors is a prerequisite step for their differentiation into osteoclasts

BMMΦ (osteoclast precursors) differentiated into TRAP^{+} multinucleated osteoclasts within 3 d in the presence of M-CSF and RANKL (Fig. 1 A). The growth of BMMΦ treated with RANKL and M-CSF was retarded on days 2 and 3 in comparison with that of M-CSF alone (Fig. 1 A, left). The levels of cyclins D1, D2, D3, and E1 and Cdk2, 4, and 6 gradually decreased after treatment with M-CSF and RANKL (Fig. 1 B). On day 3, cultures treated with M-CSF and RANKL still contained small amounts of cyclins D3 and E1 and Cdk2, 4, and 6. Using purified osteoclasts, we further examined whether mature osteoclasts express cyclins and Cdks. Purified osteoclasts (purity of osteoclasts, ~95%; Akatsu et al., 1992) failed to express cyclins D1, D2, D3, and E1 and Cdk2 and 4 (Fig. S1, available at http://www.jcb.org/cgi/content/full/jcb.200806139/DC1). Cdk6 was weakly expressed in purified osteoclasts. The expression of Cdk inhibitors p27^{KIP1} and p21^{CIP1} was reported to be up-regulated during osteoclast differentiation (Okahashi et al., 2001; Sankar et al., 2004). BMMΦ showed that the expression of p27^{KIP1} but not of p21^{CIP1} was up-regulated in the presence of RANKL (Fig. 1 B). Real-time PCR analysis confirmed that the levels of p21^{CIP1} and p27^{KIP1} mRNA in osteoclast precursors reflected the changes in p21^{CIP1} and p27^{KIP1} protein levels during their differentiation into osteoclasts (Fig. 1 C). These results suggest that cell cycle arrest in mature osteoclasts is maintained by the disappearance of cyclins and Cdks and that p27^{KIP1} rather than p21^{CIP1} is involved in RANKL-induced osteoclastic differentiation of BMMΦ.

When hydroxyurea (HU), an inhibitor of DNA replication, was added to the culture on day 0, RANKL-induced osteoclast formation was completely inhibited (Fig. 2 A). In contrast, the formation of osteoclasts was accelerated by HU when it was added on day 1 (Fig. 2 A). HU added on day 2 had no effect on osteoclast formation. BrdU is a nucleoside analogue that can be incorporated into dividing nuclei. When BrdU was added to BMMΦ cultures together with RANKL on day 0, all of the nuclei in RANKL-induced multinucleated cells were labeled with BrdU (Fig. 2 B). When BrdU was added on day 1 (1 d after treatment with RANKL), only 20% of the nuclei of multinucleated cells incorporated BrdU (Fig. 2 B). Ki67 is a marker of actively cycling cells (Gerdes et al., 1984). Most nuclei of BMMΦ

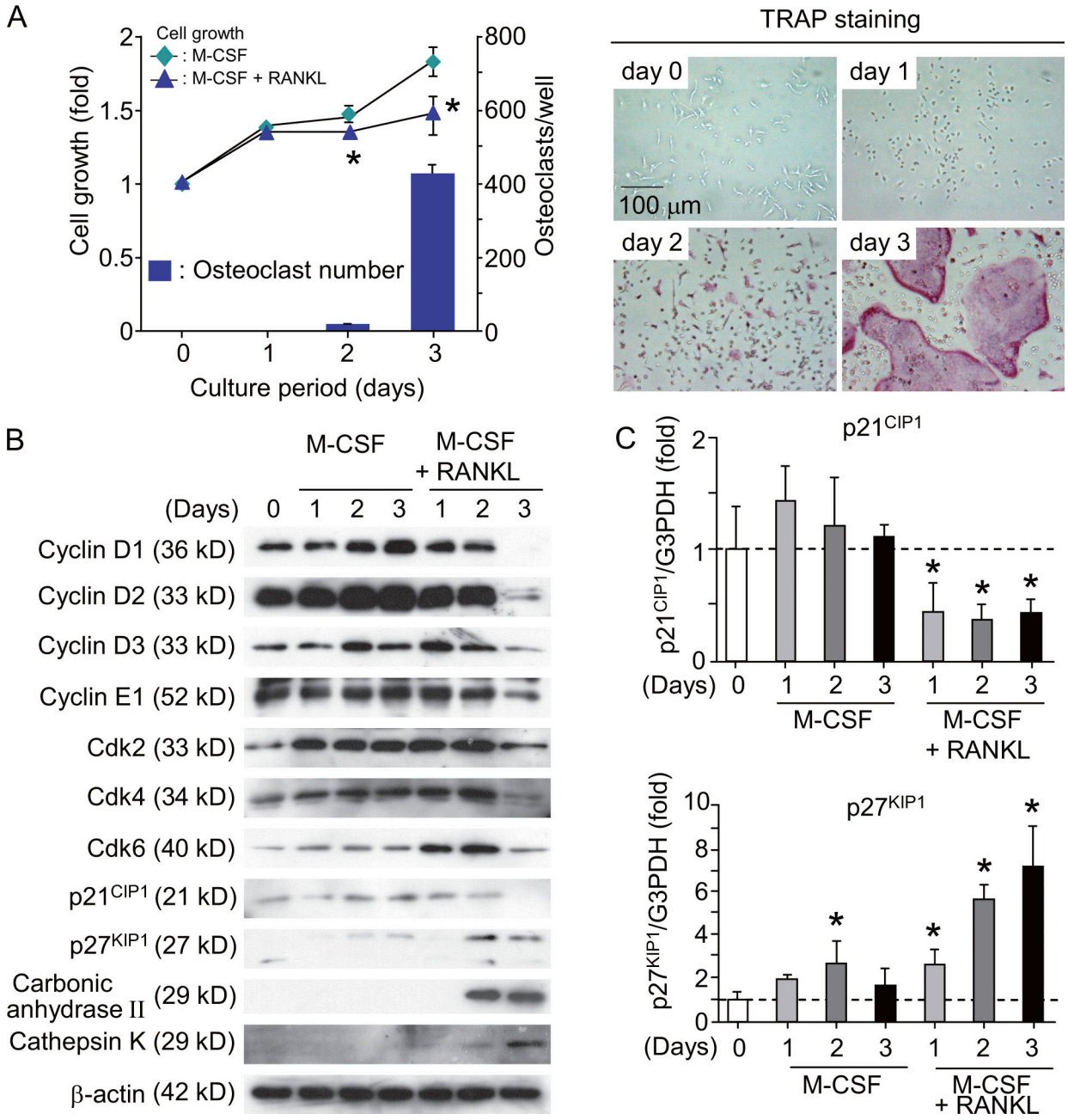

Figure 1. **Regulation of cell cycle during differentiation of BMMΦ into osteoclasts.** (A) Time course of changes in cell growth and TRAP+ osteoclast formation in BMMΦ cultures. Bone marrow cells were cultured with 10^4 U/ml M-CSF for 4 d to prepare BMMΦ. BMMΦ were further cultured with or without 100 ng/ml RANKL in the presence of 10^4 U/ml M-CSF. After culturing for the indicated periods, cell growth was measured by the AlamarBlue assay (Invitrogen) and expressed as the increase in fluorescence emission at 590 nm (excitation wavelength, 560 nm) relative to the control at day 0 (left). In the other culture treated with RANKL and M-CSF, cells were fixed and stained for TRAP (right). TRAP+ multinucleated cells containing more than three nuclei were counted as osteoclasts (bars). Results are expressed as the mean ± SD for six cultures. *, $P < 0.01$; significantly different from the culture treated with M-CSF alone. (B) Expression of cell cycle regulatory molecules and osteoclast-specific molecules in BMMΦ cultured with M-CSF or M-CSF plus RANKL. BMMΦ were cultured with 10^4 U/ml M-CSF or 10^4 U/ml M-CSF plus RANKL (100 ng/ml). After the indicated periods, cell lysates were prepared and subjected to immunoblot analyses of the indicated cell cycle regulatory molecules. Cell lysates were also analyzed for osteoclast-specific markers such as carbonic anhydrase II and cathepsin K. (C) Real-time PCR analysis of expression of $p21^{CIP1}$ and $p27^{KIP1}$ mRNAs in BMMΦ. BMMΦ were cultured with 10^4 U/ml M-CSF or10^4 U/ml M-CSF plus100 ng/ml RANKL. After the indicated periods, total RNA was extracted from cells. Expression levels of $p21^{CIP1}$ and $p27^{KIP1}$ mRNAs were estimated by quantitative real-time RT-PCR. Dashed lines indicate control levels. Results are expressed as the relative expression of $p21^{CIP1}$ and $p27^{KIP1}$ mRNAs compared to the control at day 0. *, $P < 0.05$. Error bars indicate mean ± SD for three experiments.

were stained with anti-Ki67 antibody. In contrast, all of the nuclei in osteoclasts were negative for Ki67 ($Ki67^-$; Fig. 2 C). To confirm that regulation of the cell cycle is a key determinant in osteoclast differentiation, BMMΦ were transduced with cell cycle regulatory molecules using a retroviral vector system. D-type cyclins are shown to associate with Cdk4 or 6 (Weinberg, 1995; Morgan, 1997; Classon and Harlow, 2002). Coexpression of cyclin D1 and Cdk4 in BMMΦ suppressed osteoclast formation

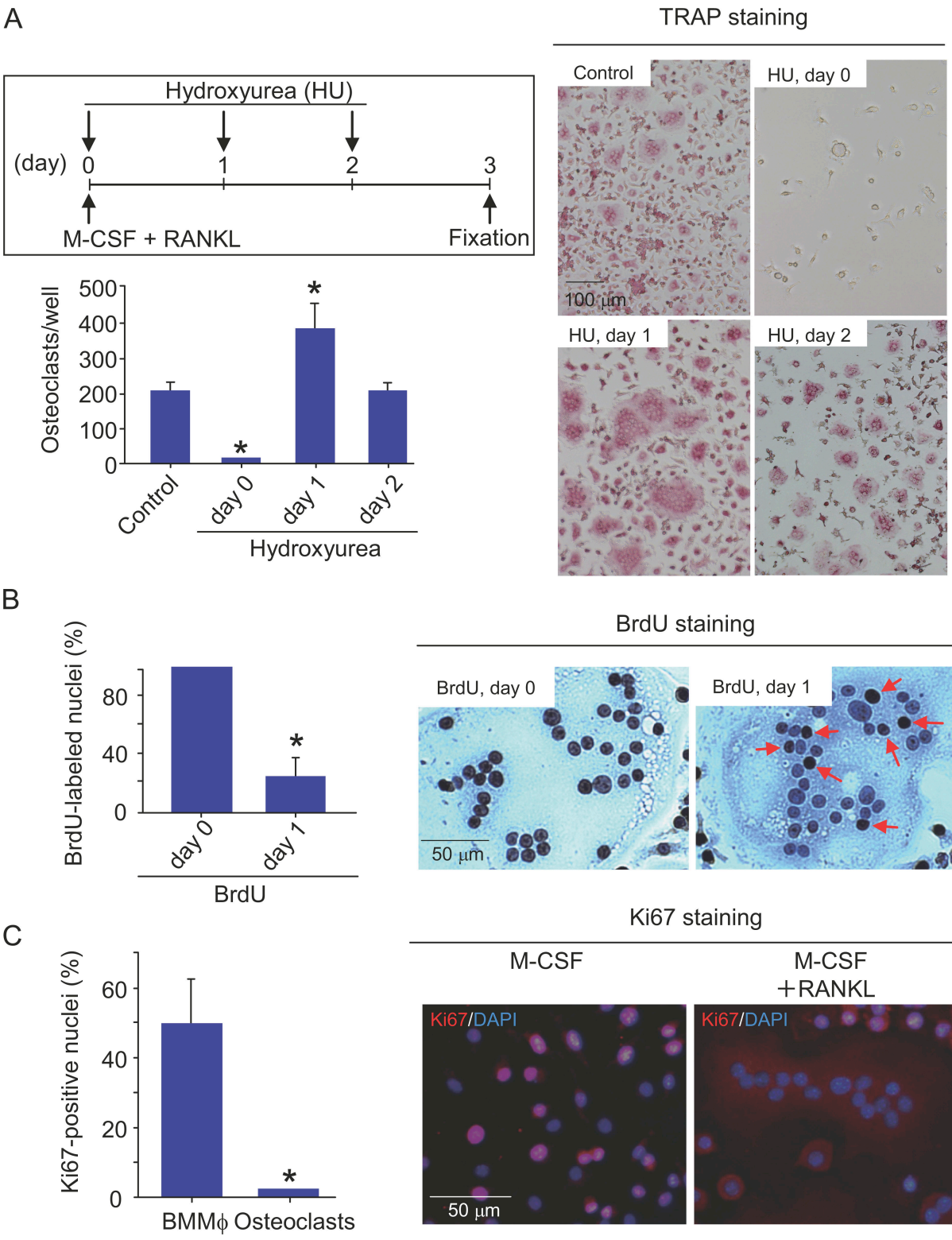

Figure 2. **Relationship between cell cycle progression and arrest in BMMΦ during differentiation into osteoclasts.** (A) Effect of HU on osteoclastic differentiation of BMMΦ. The experimental protocol is illustrated in the top left. BMMΦ were cultured with 10^4 U/ml M-CSF and100 ng/ml RANKL. 100 μM HU was added to the culture on days 0, 1, or 2. After culturing for 3 d, cells were fixed and stained for TRAP (right). $TRAP^+$ multinucleated cells containing more than three nuclei were counted as osteoclasts (bottom left). *, $P < 0.01$; significantly different from the culture incubated without HU. (B) Nuclear labeling of osteoclasts with BrdU. BMMΦ were cultured with10^4 U/ml M-CSF and100 ng/ml RANKL. 10 nM BrdU was added to the culture on days 0 and 1. After culturing for 3 d, cells were fixed and stained with antibodies against BrdU (right). Arrows indicate $BrdU^+$ nuclei in RANKL-induced multinucleated cells in cultures treated with BrdU on day 1. $BrdU^+$ and $BrdU^-$ nuclei in multinucleated cells containing more than three nuclei were counted. Percentages of nuclei labeled with BrdU were determined (left). *, $P < 0.01$; significantly different from the culture treated with BrdU on day 0. (C) Immunostaining of Ki67 in BMMΦ and osteoclasts. BMMΦ were cultured with 10^4 U/ml M-CSF and 100 ng/ml RANKL for 3 d to produce

induced by RANKL and M-CSF, whereas the expression of $p27^{KIP1}$ stimulated it (Fig. S2, A and B, available at http://www.jcb.org/cgi/content/full/jcb.200806139/DC1). These results suggest that cell cycle progression and subsequent withdrawal in osteoclast precursors are required for their differentiation into osteoclasts in vitro. The committed osteoclast precursors were named cell cycle–arrested QuOPs.

RANK-mediated signals may switch on the cell cycle arrest in osteoclast progenitors. To address this issue, primary osteoblasts were infected with a retrovirus carrying cDNA for RANK (Fig. S2 C). Neither down-regulation of cyclin D1 and Cdk4 expression nor up-regulation of $p27^{KIP1}$ expression was observed in RANK-transfected osteoblasts, even in the presence of RANKL. Osteoblasts expressing functional RANK proliferated similarly in the presence and absence of RANKL (Fig. S2 C). These results suggest that RANKL-induced cell cycle arrest is cell type specific.

BrdU labeling of osteoclasts in vivo

We next examined in vivo labeling of nuclei of osteoclasts with BrdU. BrdU in 1 mg/ml drinking water was administered for 1 wk to mice at different developmental stages, and the incorporation of BrdU into the nuclei of osteoclasts was evaluated in tibiae (Fig. 3). When pregnant mice at 13.5 d postcoitum (embryonic day 13.5 [E13.5]) were given BrdU in drinking water for 1 wk, ∼50% of the nuclei of osteoclasts in newborn mice were labeled with BrdU. Similarly, 3- and 7-wk-old mice were given BrdU in drinking water for 1 wk. About 30% of the nuclei of osteoclasts were labeled with BrdU in 4-wk-old mice. In contrast, most nuclei of osteoclasts were BrdU negative ($BrdU^-$) in 8-wk-old mice. Thus, the BrdU labeling of osteoclasts was inversely correlated with the growth of mice (Fig. 3 A). We then examined the lifespan of QuOPs in adult mice. When 7-wk-old mice were given BrdU for an additional 7 wk, only 50% of the nuclei of osteoclasts were labeled with BrdU (Fig. 3 B). Most of the bone marrow cells around osteoclasts were BrdU positive ($BrdU^+$) in mice treated with BrdU for 7 wk. Previous studies have shown that the lifespan of osteoclasts is 2–4 wk in humans and mice (Kodama et al., 1993; Riggs and Parfitt, 2005). These results suggest that the lifespan of QuOPs is at least 4 wk longer.

Differentiation of QuOPs into osteoclasts in vivo

We next examined whether osteoclasts are formed from cell cycle–arrested QuOPs in response to several stimuli. Osteoclasts are totally absent in $RANKL^{-/-}$ mice. Injection of RANKL into $RANKL^{-/-}$ mice induces osteoclasts along bone surfaces (Yamamoto et al., 2006). We first examined whether RANKL-induced osteoclasts are formed from QuOPs in $RANKL^{-/-}$ mice. RANKL (15 µg/injection) was administered i.p. into 3-wk-old $RANKL^{-/-}$ mice for 2 d (one injection/day; Fig. 4, A and B). BrdU was also i.p. injected into $RANKL^{-/-}$ mice (1 mg/injection/day) because toothless $RANKL^{-/-}$ mice were maintained with a water-containing paste diet. Osteoclasts were totally absent in tibiae of $RANKL^{-/-}$ mice (Fig. 4 A, top). The injection of RANKL into $RANKL^{-/-}$ mice generated many $TRAP^+$ cells in tibiae (Fig. 4 A, bottom). $BrdU^+$ nuclei were similarly observed in chondrocytes in growth plates in $RANKL^{-/-}$ mice injected with RANKL (Fig. 4, A [middle] and B [left]). Although many multinucleated osteoclasts were generated by the injection, >70% of the nuclei in the osteoclasts did not incorporate BrdU (Fig. 4, A and B, right). This suggests that RANKL induced the differentiation of preexisting QuOPs in bone tissues into osteoclasts in $RANKL^{-/-}$ mice.

M-CSF is believed to be involved in the proliferation as well as differentiation of osteoclast progenitors in mice. Therefore, we examined whether M-CSF–induced osteoclasts are formed from QuOPs in M-CSF–deficient op/op mice. M-CSF (2×10^6 U/injection) and BrdU (1 mg/injection) were injected i.p. into 3-wk-old op/op mice for 7 d (one injection/day; Fig. 4, C and D). Most of the nuclei of chondrocytes (∼95%) in growth plates were labeled with BrdU in op/op mice with or without M-CSF treatment because of the long period (7 d) of BrdU administration (Fig. 4, C [middle] and D [left]). Osteoclasts are hardly detected in 3-wk-old op/op mice (Fig. 4 C, top). The injection of M-CSF into op/op mice generated many $TRAP^+$ cells in contact with bone surfaces of tibiae (Fig. 4 C, bottom). Interestingly, only 15% of nuclei in M-CSF–induced osteoclasts incorporated BrdU in op/op mice (Fig. 4, C [right] and D [right]), suggesting that most osteoclasts were formed from QuOPs in response to M-CSF in op/op mice. These results also suggest that M-CSF as well as RANKL is not involved in the appearance of QuOPs in mice.

We further examined whether the differentiation of QuOPs into osteoclasts is linked to the regulation of calcium metabolism in wild-type mice. 7-wk-old mice were fed a low calcium diet for 3 d to induce osteoclastic bone resorption with the administration of BrdU in drinking water. The number of osteoclasts in tibiae and serum activity of TRAP5b, a marker of osteoclastic bone resorption, were significantly increased in the mice fed a low calcium diet (Fig. S3, available at http://www.jcb.org/cgi/content/full/jcb.200806139/DC1). However, the percentage of $BrdU^+$ nuclei in osteoclasts remained unchanged. These results suggest that osteoclasts produced by feeding on a low calcium diet are formed from QuOPs.

Identification of QuOPs as 5-FU–insensitive cells

The aforementioned data suggest that, like hemopoietic stem cells, cell cycle–arrested QuOPs should be resistant to 5-FU that induces apoptosis of cells having high proliferative potential

osteoclasts. (right) BMMΦ and BMMΦ treated with M-CSF and RANKL for 3 d were stained with anti-Ki67 antibody (red), and the nuclei were also labeled with DAPI (blue). (left) Percentages of Ki67-positive nuclei in BMMΦ and RANKL-induced osteoclasts were determined. Results are expressed as the mean ± SD for three cultures. *, $P < 0.01$; significantly different from the BMMΦ.

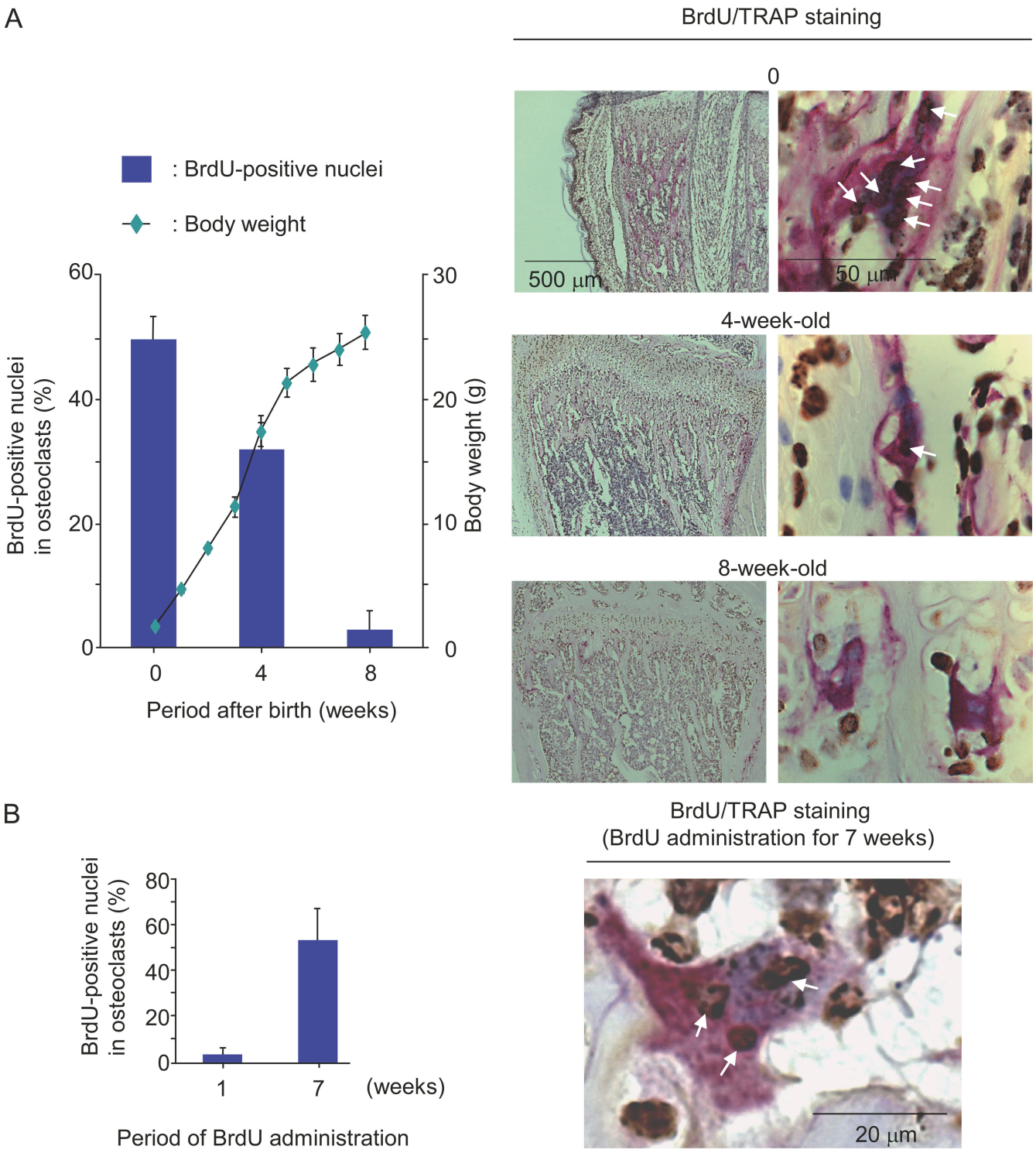

Figure 3. **Incorporation of BrdU into nuclei of osteoclasts in vivo.** (A) BrdU incorporation into nuclei in osteoclasts at different growth stages of mice. Pregnant mice at E13.5 and 3- and 7-wk-old mice were given 1 mg/ml BrdU in drinking water for 1 wk. Newborn, 4- , and 8-wk-old mice administered with BrdU for 1 wk were killed, and tibiae were recovered. Sections of tibiae were prepared and double stained for TRAP (red) and BrdU (brown). Arrows indicate the $BrdU^+$ nuclei in osteoclasts (right). $BrdU^+$ and $BrdU^-$ nuclei in osteoclasts were counted, and percentages of $BrdU^+$ nuclei in osteoclasts were determined (left). Changes in the body weight of mice are shown. (B) BrdU incorporation into nuclei in osteoclasts in adult mice. 7-wk-old mice were given 1 mg/ml BrdU in drinking water for 7 wk. Tibiae were recovered and subjected to TRAP and BrdU staining. Arrows indicate $BrdU^+$ nuclei in osteoclasts (right). Percentages of $BrdU^+$ nuclei in osteoclasts were determined (left). Results are expressed as the mean ± SD for three animals.

(Heissig et al., 2002; Arai et al., 2004). We then examined the effects of 5-FU on the differentiation of QuOPs into osteoclasts in mice (Fig. 5). 7-wk-old mice were injected i.v. with 5-FU (250 mg/kg body weight). The number of bone marrow cells was markedly decreased on day 6 after the injection (Fig. 5 A). Mice pretreated with 5-FU for 6 d were i.p. given

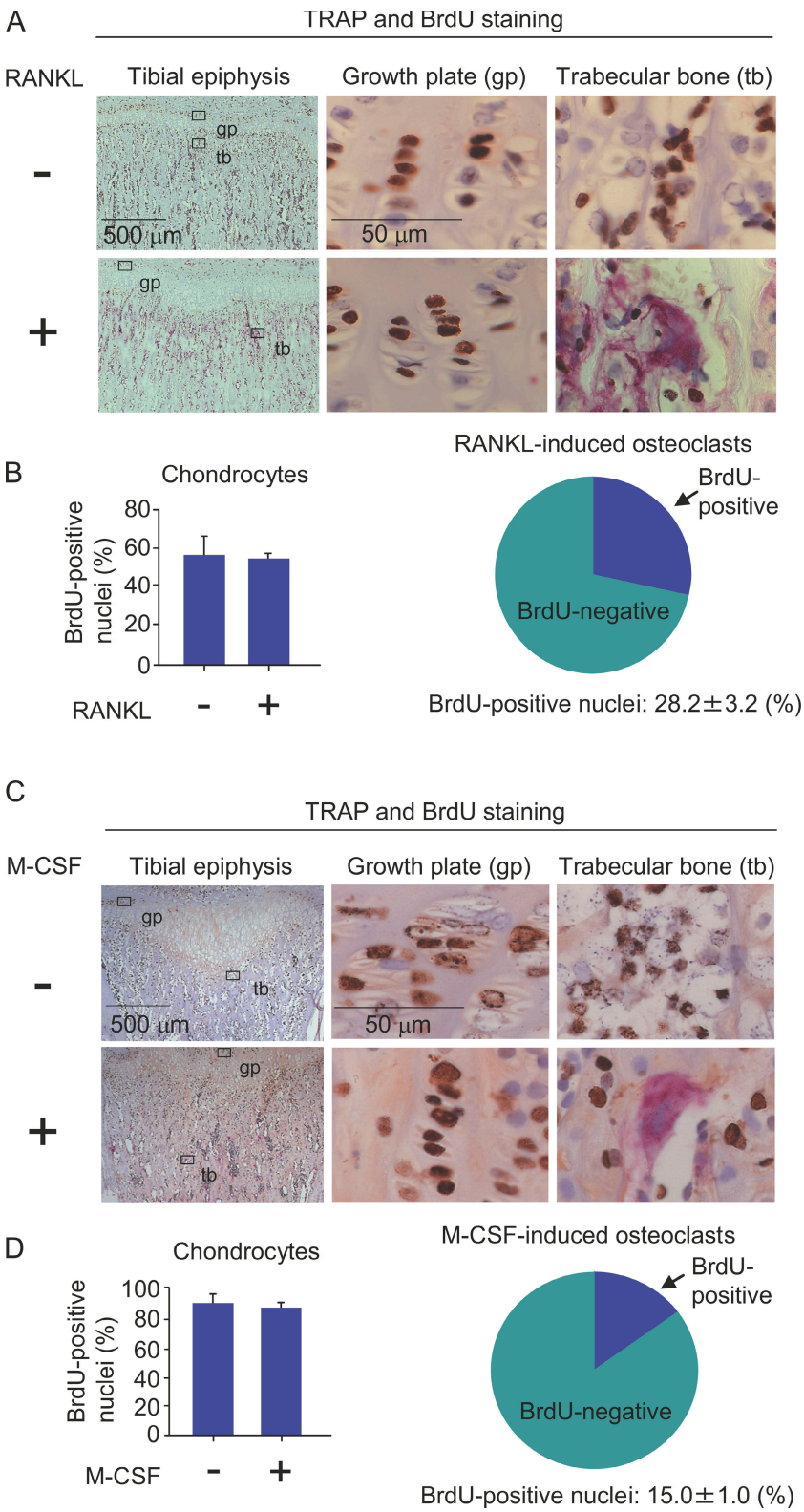

Figure 4. **Effects of RANKL and M-CSF on the incorporation of BrdU into nuclei of osteoclasts.** (A and B) Administration of RANKL to RANKL$^{-/-}$ mice. 3-wk-old RANKL$^{-/-}$ mice were i.p. injected with RANKL (15 μg/injection/day) together with BrdU (1 mg/injection/day) for 2 d. The first injection of BrdU was performed 3 h before the first injection of RANKL. 24 h after the final injection, the tibiae were recovered. (A) Sections of tibiae were prepared and double stained for TRAP (red) and BrdU (brown). Portions of the epiphyseal growth plate (middle) and trabecular bone (right) were observed at a higher magnification. (top) Osteoclasts were totally absent in RANKL$^{-/-}$ mice. (bottom) The administration of RANKL to RANKL$^{-/-}$ mice induced osteoclasts to form in trabecular bones. (B, left) BrdU$^+$ and BrdU$^-$ nuclei of chondrocytes in growth plates were counted, and percentages of BrdU$^+$ nuclei in chondrocytes were calculated. (right) BrdU$^+$ and BrdU$^-$ nuclei of RANKL-induced osteoclasts were counted, and percentages of BrdU$^+$ nuclei in the osteoclasts were calculated. (C and D) Administration of M-CSF to op/op mice. 3-wk-old op/op mice were i.p. injected with M-CSF (2×10^6 U/injection/day) together with BrdU (1 mg/injection/day) daily for 7 d. The first injection of BrdU was performed 3 h before the first injection of M-CSF. 24 h after the final injection, the tibiae were removed from the mice. (C) Sections of tibiae were prepared and double stained for TRAP (red) and BrdU (brown). Portions of epiphyseal growth plate (middle) and trabecular bone (right) were observed at a higher magnification. (top) Osteoclasts were totally absent in the tibiae of 3-wk-old op/op mice. (bottom) The administration of M-CSF to op/op mice induced osteoclasts to form in trabecular bones. (D, left) BrdU$^+$ and BrdU$^-$ nuclei of chondrocytes in growth plates were counted and percentages of BrdU$^+$ nuclei in chondrocytes were calculated. (right) BrdU$^+$ and BrdU$^-$ nuclei of M-CSF–induced osteoclasts were counted, and percentages of BrdU$^+$ nuclei in the osteoclasts were calculated. The results are expressed as the mean ± SD for three animals.

2MD (2-methylene-19-nor-1α,25(OH)$_2$D$_3$; a potent analogue of 1α,25(OH)$_2$D$_3$; 50 pmol/injection) for an additional 2 d with BrdU administered in drinking water. Expectedly, 2MD injected into 5-FU–pretreated mice significantly increased the number of TRAP$^+$ osteoclasts in tibiae even under myelosuppressive conditions in bone (Fig. 5 B). The percentage of BrdU$^+$ nuclei in osteoclasts remained unchanged by the injection (Fig. 5 B). Calcium concentrations and TRAP5b activities in serum were significantly increased in response to 2MD in 5-FU–pretreated mice (Fig. 5 C). These results suggest that 2MD-induced osteoclasts were formed from 5-FU–insensitive QuOPs.

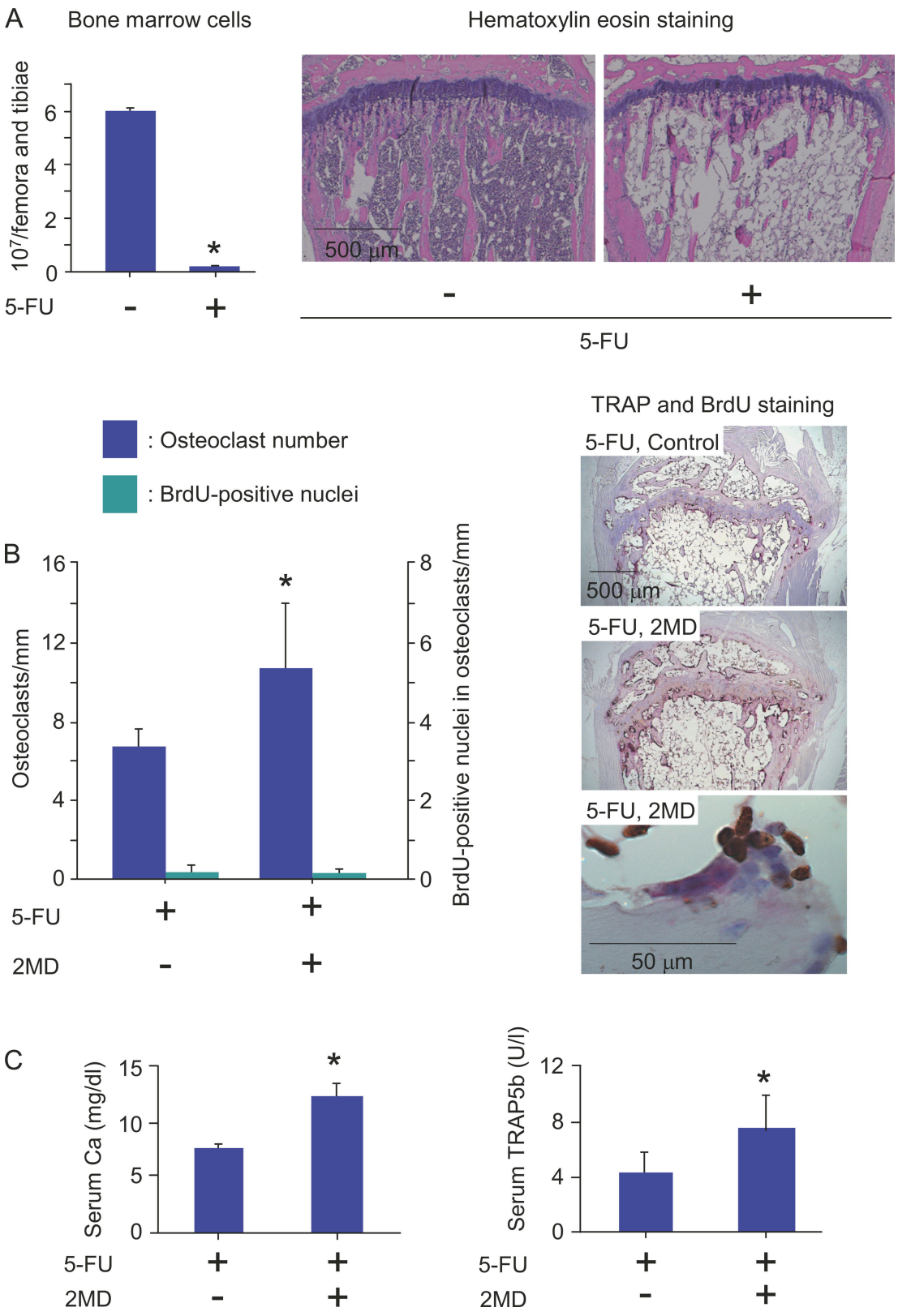

Figure 5. **Effects of 5-FU administration on osteoclastic bone resorption induced by 2MD.** (A) Effects of 5-FU administration on hemopoietic cells in bone marrow. 7-wk-old mice were i.v. injected with 5-FU (250 mg/kg body weight). (left) On day 6 after injection, bone marrow cells obtained from the femora and tibiae were counted. Tibiae were also recovered from other 5-FU–treated and control mice. (right) Sections of tibiae were prepared and stained with hematoxylin-eosin. *, $P < 0.01$; significantly different from control mice. (B and C) Effects of 2MD administration on differentiation of QuOPs into osteoclasts. 7-wk-old mice were i.v. injected with 5-FU (250 mg/kg body weight). From day 6 after injection, mice were i.p. injected with 2MD (50 pmol/injection/day) or vehicle for an additional 2 d with 1 mg/ml BrdU given in their drinking water. (B, right) The mice were killed, and blood and tibiae were recovered. Sections of tibiae were prepared and double stained for TRAP and BrdU. $TRAP^+$ osteoclasts and $BrdU^+$ and $BrdU^-$ nuclei in osteoclasts

Identification of QuOPs as double-positive cells for c-Fms and RANK in bone

The aforementioned data suggest that QuOPs are resistant to 5-FU and are present in bone. QuOPs as well as osteoclasts are expected to express both M-CSF receptors (c-Fms) and RANKL receptors (RANK; Miyamoto et al., 2000). Next, we examined whether the administration of 5-FU alters the population of c-Fms$^+$/RANK$^+$ cells (c-Fms and RANK double-positive cells) in the bone marrow. 5-FU was i.v. injected into 7-wk-old mice. On day 8 after injection, bone marrow cells were collected and analyzed with a flow cytometer (Fig. 6). MOMA-2$^+$/CD11b$^+$ cells (monocytes/macrophages) decreased in number with the injection (Fig. 6 A, left). In contrast, 5-FU increased the Fms$^+$/RANK$^+$ cell population in the bone marrow cells (Fig. 6 A, right), suggesting that c-Fms$^+$/RANK$^+$ cells were cell cycle arrested. We then examined whether MOMA-2$^+$/CD11b$^+$ cells and c-Fms$^+$/RANK$^+$ cells can differentiate into osteoclasts without proliferating. MOMA-2$^+$/CD11b$^+$ cells differentiated into TRAP$^+$ osteoclasts in response to M-CSF and RANKL in the absence but not presence of HU (Fig. 6 B). In contrast, c-Fms$^+$/RANK$^+$ cells differentiated into TRAP$^+$ cells even in the presence of HU (Fig. 6 B).

Finally, we tried to detect c-Fms$^+$/RANK$^+$ cells in bone tissues in RANKL$^{-/-}$ mice because QuOPs but not osteoclasts are present in RANKL$^{-/-}$ mice (Fig. 4, A and B). Many mononuclear cells double positive for c-Fms and RANK (c-Fms$^+$/RANK$^+$ cells; Fig. 7 A, yellow) were detected along the surface of proximal tibiae in wild-type mice (Fig. 7 A, left, arrows). Double-positive multinucleated cells were also observed in the same regions (Fig. 7 A, asterisk). These multinucleated cells appeared to be osteoclasts. QuOPs were shown to be resistant to 5-FU treatment (Figs. 5 and 6). Coincidently, c-Fms$^+$/RANK$^+$ mononuclear cells were also detected even after treatment with 5-FU (Fig. 7 A, bottom left). c-Fms$^+$/RANK$^+$ mononuclear cells were detected along the surface of proximal tibiae in the RANKL$^{-/-}$ mice (Fig. 7 A, right). Because most RANK$^+$ cells expressed c-Fms in RANKL$^{-/-}$ mice, we examined the expression of Ki67, a marker of actively cycling cells. Most of the RANK$^+$ cells (94%) were negative for Ki67 in RANKL$^{-/-}$ mice (Fig. 7 A, bottom right).

Osteoblasts may be involved in the maintenance of QuOPs in bone tissues. The distribution of ALP$^+$ osteoblasts was compared with that of RANK$^+$ cells in RANKL$^{-/-}$ mice (Fig. 7 B). ALP$^+$ cells were distributed along the bone surface in trabecular bone. Hypertrophic chondrocytes also expressed ALP (Fig. 7 B, inset). The distribution of RANK$^+$ cells was quite similar to that of ALP$^+$ cells in the trabecular bone area. Higher magnification of this area showed that RANK$^+$ cells were always present in the vicinity of ALP$^+$ osteoblasts. The distribution of osteoblasts and proliferating cells adjacent to osteoblasts was determined using another cell proliferation marker, proliferating cell nuclear antigen. Most of the cells adjacent to ALP$^+$ cells were negative for proliferating cell nuclear antigen in RANKL$^{-/-}$ mice (unpublished data). These results suggest that osteoblasts are involved in the maintenance of QuOPs in bone.

Discussion

In this study, we have demonstrated characteristics of cell cycle–arrested QuOPs as the committed osteoclast precursors in vivo. QuOPs had a quite long lifespan associated with resistance to 5-FU treatment and promptly differentiated into osteoclasts without cell cycle progression in response to all the experimental conditions tested. Mononuclear cells expressing c-Fms and RANK but not Ki67 (possibly QuOPs) were also detected along bone surfaces in the vicinity of osteoblasts in RANKL$^{-/-}$ mice. These results suggest that osteoblasts may play a role in maintaining QuOPs for a long period in an undifferentiated state.

Identification of QuOPs as osteoclast precursors

Cell cycle withdrawal of BMMΦ during their differentiation into osteoclasts appeared to be associated with down-regulation of cyclins and Cdks and up-regulation of p27^{KIP1}. Coexpression of cyclin D1 and Cdk4 in BMMΦ suppressed osteoclast formation, whereas the expression of p27^{KIP1} stimulated it. In addition, Okahashi et al. (2001) reported that RANKL up-regulated both p27^{KIP1} and p21^{CIP1} expression in osteoclast precursors. Sankar et al. (2004) showed that p27^{KIP1} and p21^{CIP1} double-knockout mice developed osteopetrosis with fewer osteoclasts. Forced expression of functional RANK in osteoblasts failed to induce cell cycle withdrawal. These results suggest that cell cycle arrest induced by RANKL is essential for osteoclastic differentiation and is peculiar to osteoclast precursors.

QuOPs are proposed to express both c-Fms and RANK. In fact, c-Fms$^+$/RANK$^+$ cells isolated from bone marrow differentiated into osteoclasts even in the presence of HU. We further characterized the c-Fms$^+$/RANK$^+$ cells isolated from bone marrow of wild-type mice in more detail (Fig. S4, available at http://www.jcb.org/cgi/content/full/jcb.200806139/DC1). Immunohistochemical staining showed that most of the c-Fms$^+$/RANK$^+$ cells were negative for F4/80 (Fig. S4 A). c-Fms$^+$/RANK$^+$ cells were cultured with lipopolysaccharide (LPS) together with M-CSF for 3 d, and the appearance of macrophages was evaluated by F4/80 staining. The number of F4/80-positive cells was not increased, even in cultures treated with LPS (Fig. S4 A). Both F4/80$^+$ cells and RANK$^+$ cells were detected in tibiae in wild-type mice, but cells double positive for RANK and F4/80 were rarely observed (Fig. S4 B). Phagocytic activity of c-Fms$^+$/RANK$^+$ cells were much lower than that of BMMΦ (Fig. S4 C). c-Fms$^+$/RANK$^+$ cells were further cultured with LPS together with M-CSF for 3 d. The number of bead-positive cells was slightly increased from the initial value, but most of the cells (≥80%) remained as nonphagocytic cells (Fig. S4 C). The ability of c-Fms$^+$/RANK$^+$ cells to differentiate into dendritic

were counted. (left) Percentages of BrdU$^+$ nuclei in osteoclasts were calculated. (C) Serum calcium concentrations and TRAP5b activities were determined in 5-FU–treated mice injected with and without 2MD. (B and C) *, $P < 0.05$; significantly different from the 5-FU–injected mice. Results are expressed as the mean ± SD for three animals.

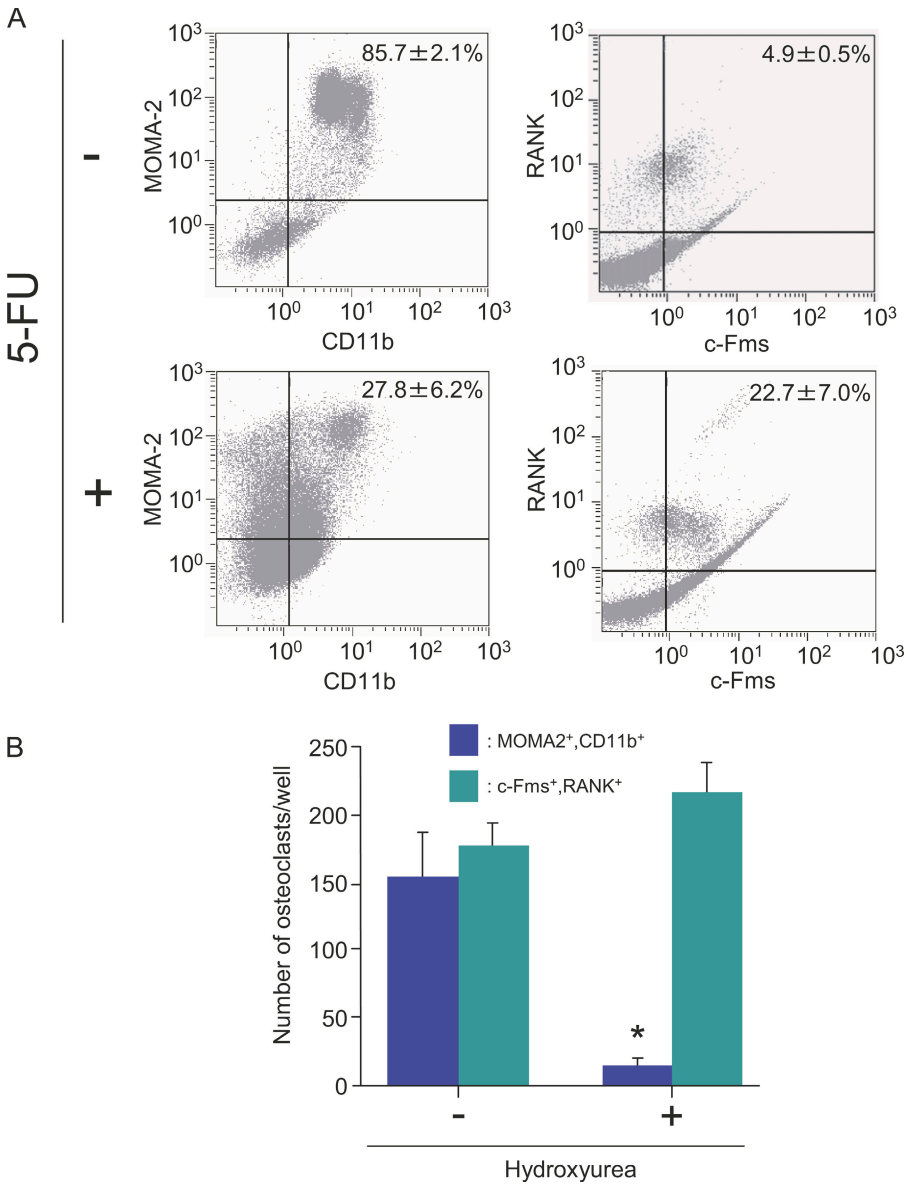

Figure 6. **Effects of 5-FU on changes in hemopoietic cell populations.** (A) Flow cytometric analysis of bone marrow cells. 7-wk-old mice were injected with vehicle (top) or 5-FU (250 mg/kg body weight; bottom). 8 d after the injection, mice were killed. Bone marrow cells prepared from tibiae were analyzed for the expression of MOMA-2 and CD11b (left) and c-Fms and RANK (right). The numbers in the top right corners indicate percentages of MOMA-2$^+$/CD11b$^+$ cells or of c-Fms$^+$/RANK$^+$ cells among all bone marrow cells. Results are expressed as the mean ± SD for three animals. (B) Effects of HU on osteoclast formation. MOMA-2$^+$/CD11b$^+$ cells and c-Fms$^+$/RANK$^+$ cells were isolated from bone marrow of wild-type mice by magnetic cell sorting and cultured in the presence of 10^4 U/ml M-CSF and 100 ng/ml RANKL. 70 μM HU was added to some cultures. After 6 d of culture, cells were fixed and stained for TRAP. TRAP$^+$ multinucleated cells containing more than three nuclei were counted as osteoclasts. Results are expressed as the mean ± SD for six cultures. *, $P < 0.01$; significantly different from the culture incubated without HU.

cells was much lower than that of BMMΦ (Fig. S4 D). In contrast to BMMΦ, c-Fms$^+$/RANK$^+$ cells failed to proliferate in response to M-CSF (unpublished data). These results suggest that c-Fms$^+$/RANK$^+$ cells isolated from bone marrow are committed precursors in an osteoclast lineage.

We previously reported that postmitotic osteoclast precursors were formed in cocultures of osteoblasts and bone marrow cells (Tanaka et al., 1993; Takahashi et al., 1994). Postmitotic osteoclast precursors differentiated into osteoclasts even in the presence of HU, suggesting that the postmitotic osteoclast precursors are QuOPs. c-Fms$^+$/RANK$^+$ cells were also formed in the cocultures (unpublished data). These results suggest that osteoblasts may play a role in the differentiation of hematopoietic progenitors into QuOPs.

In vivo characterization of QuOPs

Percentages of BrdU$^+$ nuclei in osteoclasts decreased with the growth of mice. When 7-wk-old mice were given BrdU for an additional 7 wk, only 50% of the nuclei of osteoclasts were labeled with BrdU. The lifespan of osteoclasts is reported to be 2–4 wk in humans and mice (Kodama et al., 1993; Riggs and Parfitt, 2005). These results suggest that the pool of QuOPs is much smaller in growing mice than adult mice and that the lifespan of QuOPs is quite longer than that of osteoclasts. In fact, most osteoclasts were formed from QuOPs in response to all the stimuli, such as the administration of RANKL in RANKL$^{-/-}$ mice, the administration of M-CSF in op/op mice, the feeding of a low calcium diet in wild-type mice, and the administration of 2MD in 5-FU–pretreated mice. These results also suggest that neither M-CSF nor RANKL is involved in the proliferation of osteoclast progenitors and their differentiation into QuOPs in vivo.

Although M-CSF regulates growth and differentiation of monocyte/macrophage lineage cells in vivo, M-CSF–independent macrophages are shown to still be present in op/op mice (Naito, 1993; Wiktor-Jedrzejczak and Gordon, 1996). QuOPs may be

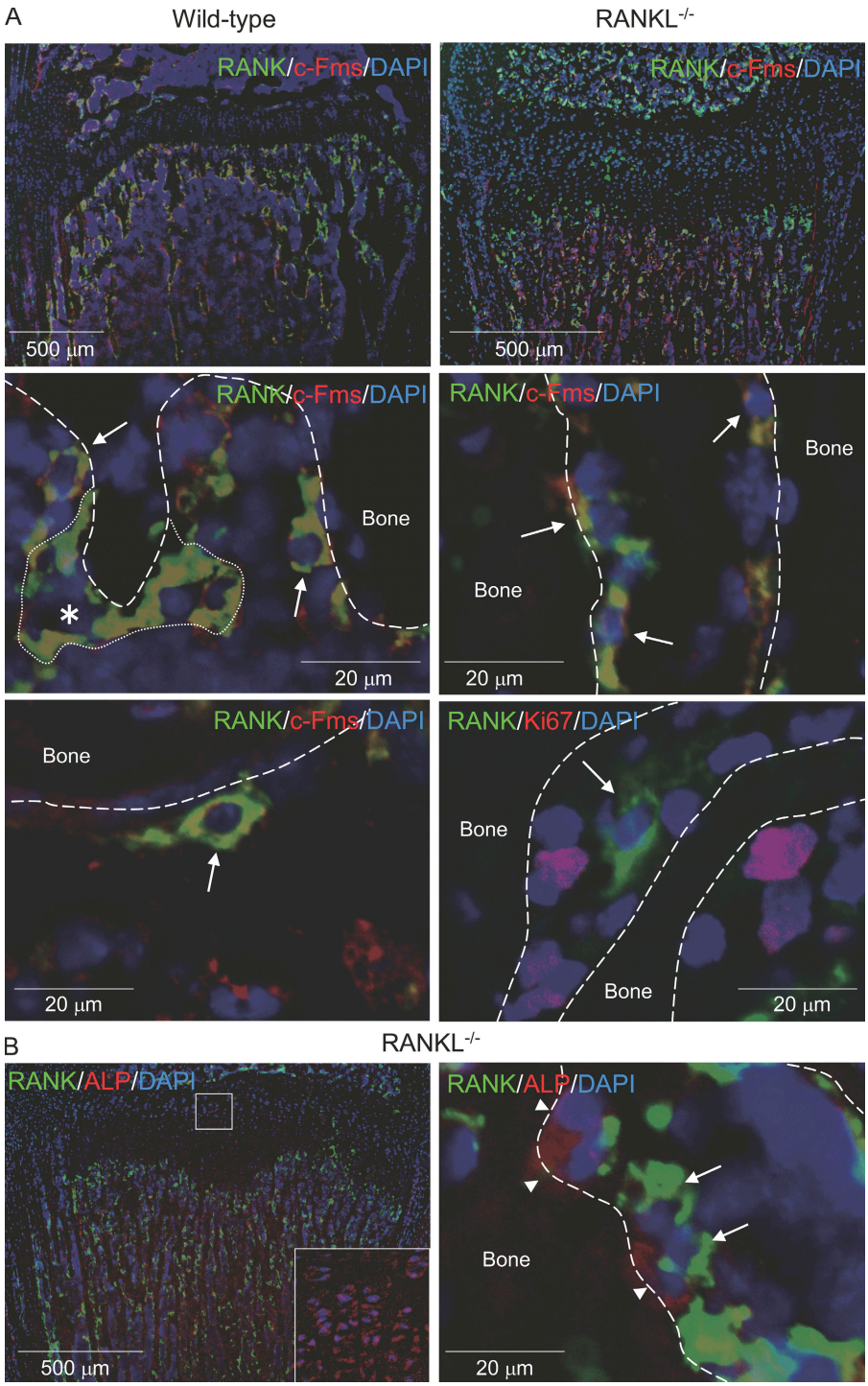

Figure 7. **Localization of QuOPs in bone.** (A) Localization of c-Fms$^+$/RANK$^+$ and Ki67$^+$ cells. Tibiae were recovered from 7-wk-old wild-type and 3-wk-old RANKL$^{-/-}$ mice. Sections of tibiae were prepared and subjected to double staining of RANK (green) and c-Fms (red; top and middle). Nuclei were labeled with DAPI (blue). Top panels show low power views of the specimens, and middle and bottom panels show high power views. (middle) The asterisk indicates a multinucleated osteoclast, which is surrounded by a small dotted line, and arrows indicate mononuclear cells double positive for RANK and c-Fms (yellow). Tibiae were also recovered from 7-wk-old wild-type mice pretreated with 5-FU for 6 d. (bottom left) Sections of tibiae from 5-FU–treated mice were stained for RANK (green), c-Fms (red), and DAPI (blue). The arrow indicates cells double positive for c-Fms and RANK in 5-FU–treated mice. (bottom right) Sections of tibiae from RANKL$^{-/-}$ mice were also stained for RANK (green), Ki67 (red), and DAPI (blue). The arrow indicates a RANK$^+$ and Ki67$^-$ cell. Bones are indicated by dashed lines. (B) Localization of RANK$^+$ cells and ALP$^+$ cells. Sections of tibiae from RANKL$^{-/-}$ mice were subjected to staining of RANK (green), ALP (red), and DAPI (blue). Arrows and arrowheads indicate RANK$^+$ and ALP$^+$ cells, respectively. The inset shows a high power view of the boxed region.

derived from such M-CSF–independent cells in vivo. RANKL and M-CSF were required to prepare QuOPs from BMMΦ in vitro in the absence of osteoblasts. In contrast to the QuOPs in vivo, we could not maintain the QuOPs, which were formed in BMMΦ cultures for >3 d with the capability to differentiate into osteoclasts in the absence of osteoblasts (unpublished data). In addition, our preliminary experiments showed that wild-type and RANKL$^{-/-}$ osteoblasts failed to maintain QuOPs in an undifferentiated state for a long period in culture (unpublished data). These results suggest that the characteristics of QuOPs formed in cultures are somehow different from those of QuOPs in vivo.

Fischman and Hay (1962) examined the origin of osteoclasts in regenerating salamander forelimbs. Osteoclasts first appeared in the regenerating limb on day 8 after amputation. Using ^{3}H-thymidine, they showed that osteoclasts appearing in the limb are formed from precursors circulating in blood. Osteoclast precursors did not proliferate in the regenerating limb. Osteoclasts labeled with ^{3}H-thymidine were detected only when ^{3}H-thymidine was administered to the salamander 1 d before the

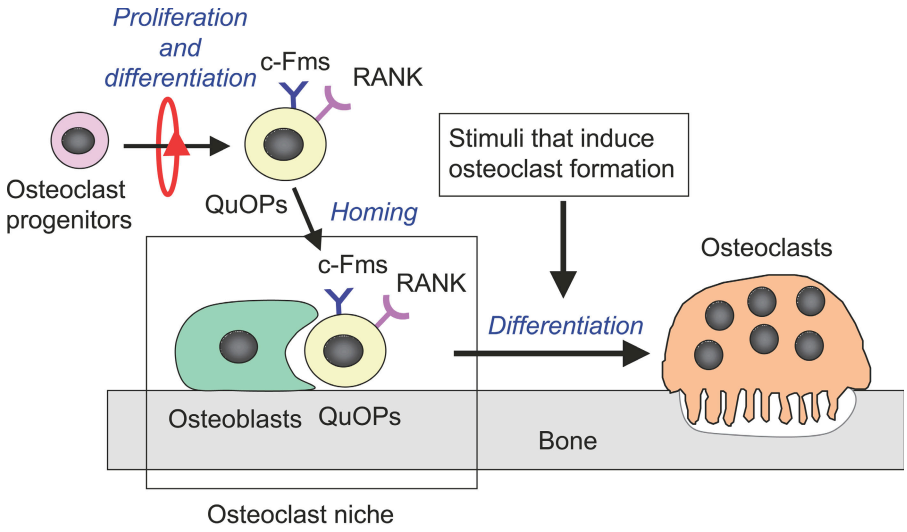

QuOPs: Cell cycle-arrested quiescent osteoclast precursors

Figure 8. **Schematic representation of osteoclast niche.** Osteoclasts differentiate from monocyte/macrophage lineage cells through two sequential cell cycle–related events. Cell cycle–arrested QuOPs are the committed precursors of osteoclasts. Osteoclast precursors proliferate and differentiate into QuOPs in hemopoietic tissues. QuOPs reach osteoclast niches prepared by osteoblasts. QuOPs differentiate into osteoclasts without cell cycle progression in response to all the stimuli that induce osteoclast formation. Osteoblasts may play a pivotal role in maintaining QuOPs for a long period in an undifferentiated state.

amputation. These results suggest that QuOPs are formed in other hemopoietic tissues.

In vivo identification of QuOPs

Using RANKL$^{-/-}$ mice, we could identify QuOPs as c-Fms^{+}/RANK^{+} cells. Most of the RANK^{+} cells were negative for Ki67 in RANKL$^{-/-}$ mice. c-Fms^{+}/RANK^{+} cells were also detected in bone tissues in wild-type mice treated with 5-FU. These results confirmed the notion that QuOPs identified as c-Fms^{+}/RANK^{+} cells in vivo are cell cycle–arrested cells. Like RANKL$^{-/-}$ mice, c-Fos knockout (c-Fos$^{-/-}$) mice exhibit severe osteopetrosis as a result of a lack of osteoclasts (Wang et al., 1992). The distribution of c-Fms^{+}/RANK^{+} cells was examined in bone tissues in c-Fos$^{-/-}$ mice (Fig. S5, available at http://www.jcb.org/cgi/content/full/jcb.200806139/DC1). Consistent with a previous study, F4/80^{+} cells were detected in proximal tibiae (Grigoriadis et al., 1994). c-Fms^{+} cells were similarly observed along the bone surface. However, RANK^{+} cells were hardly observed in bone tissues in c-Fos$^{-/-}$ mice (Fig. S5). These results suggest that c-Fos signaling is important for the differentiation of hematopoietic cells into QuOPs. The abnormal bone resorption was observed in some genetically modified mice such as tumor necrosis factor-α transgenic mice (Yao et al., 2006) and osteoprotegerin$^{-/-}$ mice (Bucay et al., 1998; Mizuno et al., 1998). Analysis of QuOPs in those mice may provide variable information on the mechanism of osteoclastogenesis.

Osteoclast niche prepared by osteoblasts

How do QuOPs recognize and settle at sites suitable for osteoclastogenesis? In preliminarily experiments, we observed that osteoclasts detected in BMP-2–induced ectopic bones are formed from circulating QuOPs (unpublished data). These results suggest that hemopoietic tissues supply QuOPs, which reach the site where osteoclasts form through the blood stream. Osteoblasts may play a role in the homing of QuOPs to bone tissues. These homing and maintenance mechanisms occur in osteoclast niches (Fig. 8). Recent studies have shown that cells of the osteoblastic lineage function as a key component of the HSC niche controlling HSC numbers (Calvi et al., 2003; Zhang et al., 2003). Osteoblasts may be involved in maintaining QuOPs as well as HSCs for a long period in a quiescent state. Unlike HSCs, QuOPs are cells with transient characteristics but without a self-renewal capacity. The role of osteoblasts in an osteoclast niche may be different from that in the HSC niche. Further studies will elucidate the molecular mechanisms of the maintenance of QuOPs in osteoclast niches.

Materials and methods

Animals and diet

6-wk-old male ddY mice, 3- and 7-wk-old male C57BL/6 mice, and pregnant C57BL/6 mice at E13.5 were obtained from Japan SLC. Cell cultures were performed using cells obtained from ddY mice. In vivo experiments were performed in C57BL/6 mice. Osteopetrotic (op/op) mice (C57BL/6) were obtained from The Jackson Laboratory. RANKL$^{-/-}$ mice (C57BL/6) were generated in one of the authors' laboratories (Kong et al., 1999). In some experiments, wild-type mice (C57BL/6), RANKL$^{-/-}$ mice, and op/op mice received i.p. injections of 2MD, RANKL (PeproTech), and M-CSF (Kyowa Hakko), respectively. 2MD was provided by M. Shimizu (Tokyo Medical and Dental University, Tokyo, Japan; Yamamoto et al., 2003). All experiments were conducted in accordance with the guidelines for studies with laboratory animals of the Matsumoto Dental University Experimental Animal Committee.

Cultures of BMMΦ

To obtain bone marrow macrophages, bone marrow cells obtained from tibiae of 6-wk-old ddY mice were cultured in α-MEM (Sigma-Aldrich) containing 10% FBS (JRH Biosciences) in the presence of 10^4 U/ml M-CSF. After culture for 16 h, nonadherent cells were harvested, and 1.5×10^5 cells were incubated with 10^4 U/ml M-CSF for 2 d in 48-well plates. Old media were replaced with fresh media containing M-CSF and further cultured for 24 h. The adherent cells were used as BMMΦ. This time point was designated as day 0 in all the experiments. BMMΦ were further cultured with or without 100 ng/ml RANKL in the presence of 10^4 U/ml M-CSF for 3 d. Some BMMΦ cultures were incubated with 100 μM HU (MP Biomedicals) or 10 nM BrdU (Sigma-Aldrich). After being cultured for the specific periods, cells were fixed and stained for TRAP (Takahashi et al., 1988). The BrdU incorporated into cells was detected by using a BrdU immunohistochemistry kit (Exalpha Biologicals). Images were obtained using A-Plan 10 ×/0.25 Ph1 and long-distance A-Plan 40 ×/0.50 Ph2 objectives (Carl Zeiss, Inc.) on a microscope (Axiovert 200; Carl Zeiss, Inc.) with a digital camera (AxioCamHRc; Carl Zeiss, Inc.). Images were captured with

AxioVision software (Carl Zeiss, Inc.). Cell growth was estimated by the cell viability AlamarBlue assay (Invitrogen).

Western blot analysis

Cells were lysed in 0.1% NP-40 lysis buffer (20 mM Tris, pH 7.5, 50 mM β-glycerophosphate, 150 mM NaCl, 1 mM EDTA, 25 mM NaF, 1 mM Na_3VO_4, 1× protease inhibitors cocktail [Sigma-Aldrich], 1× phosphatase inhibitors cocktail I [Sigma-Aldrich], and phosphatase inhibitors cocktail II [Sigma-Aldrich]). Cell lysates were electrophoresed on an SDS-PAGE gel, transferred onto a PVDF membrane (clear blot P membrane; ATTO), blotted with antibodies to specific proteins, and visualized using ECL (GE Healthcare). The following antibodies were used for primary antibodies: anti–cyclin D1 (72-13G), anti–cyclin D2 (C-17), anti-$p27^{KIP1}$ (F-8), and anti-carbonic anhydrase II (M-14) obtained from Santa Cruz Biotechnology, Inc.; anti–cyclin E1 and anti–β-actin (AC-74) obtained from Sigma-Aldrich; anti–cyclin D3 (1), anti-Cdk2 (55), and anti-$p21^{CIP1}$ (SXM30) obtained from BD; anticathepsin K (182-12G5) obtained from Daiichi Fine Chemical; and anti-Cdk4 (DCS-35) and anti-Cdk6 (K6.83) obtained from Millipore.

Real-time PCR

Total RNA was extracted from BMMΦ. cDNA was synthesized from the total RNA using reverse transcription (Rever Tra Ace; Toyobo) and subjected to a two-step PCR in the DNA Engine Opticon system (MJ Japan) using the specific primers. The fold/change ratios between test and control samples were calculated. The sequences of primers for each gene were as follows: $p21^{CIP1}$, 5′-TTGCACTCTGGTGTCTGAGC-3′ (forward) and 5′-TCTGCGCTTGGAGTGATAGA-3′ (reverse); $p27^{KIP1}$, 5′-TTGGGTCTCAGGCAAACTCT-3′ (forward) and 5′-TTACGTCTGGCGTCGAAGG-3′ (reverse); and glyceraldehyde-3-phosphate dehydrogenase (G3PDH), 5′-ACCACAGTCCATGCCATCAC-3′ (forward) and 5′-TCCACCACCCTGTTGCTGTA-3′ (reverse).

In vivo labeling of nuclei with BrdU

Wild-type mice were given 1 mg/ml BrdU in drinking water. Osteopetrotic mice received i.p. injections of BrdU (1 mg/head/day) because they were fed a water-containing paste diet. After the administration of BrdU for the indicated period, mice were killed, and tibiae were removed and subjected to BrdU staining. Some specimens were double stained for TRAP and BrdU.

Immunohistochemical analysis

Cultured cells were fixed and incubated with anti-Ki67 antibody (Novocastra Laboratories) followed by a rhodamine-conjugated secondary anti–rabbit IgG (GE Healthcare). Cells were also stained with DAPI (Vector Laboratories). Images were obtained using a long-distance A-Plan 40 ×/0.50 Ph2 objective on a microscope (Axiovert 200) with a digital camera (AxioCamHRc). Images were captured with AxioVision software. Figure construction of images was performed using the Photoshop software (Adobe).

The tibial sections were subjected to staining for TRAP and BrdU (anti-BrdU antibodies; BD) and counterstaining with hematoxylin. $TRAP^+$ osteoclasts and $BrdU^+$ and $BrdU^-$ nuclei in osteoclasts were counted in eight images of 0.036 mm^2 (220 × 164 µm) located under the growth plate (trabecular bone regions). The bone morphometric analysis was performed using an analytic software (TRI/3D-BON; Ratoc System Engineering Co., Ltd.). For immunofluorescent staining, tibiae were frozen in hexane using a cooling apparatus (PSL-1800; Tokyo Rikakikai Co., Ltd.) and embedded in a 5% carboxymethyl cellulose gel. The 5-µm-thick sections of nondecalcified tibiae were prepared using Kawamoto's film method (cryofilm transfer kit; Fintec Co., Ltd.) and fixed in ice-cold 5% acetic acid in ethanol (Kawamoto and Shimizu, 2000). The sections were subjected to staining for c-Fms, RANK, ALP, and Ki67 using specific antibodies (biotinylated anti-RANK; R&D Systems), anti–c-Fms (Millipore), and anti-ALP (generated in one of the authors' laboratories; Oda et al., 1999). Biotinylated antibodies were visualized with a Tyramide Signal Amplification kit for FITC (PerkinElmer). Rhodamine-conjugated anti–rabbit IgG was used as the secondary antibody. The sections were also subjected to DAPI staining. Images were obtained using Plan-Neofluar 5 ×/0.15 and Plan-Neofluar 40 ×/0.75 objectives (Carl Zeiss, Inc.) on a microscope (Axioplan 2 imaging; Carl Zeiss, Inc.) with a digital camera (AxioCamHRc). Images were captured with AxioVision software. Figure construction of images was performed using the Photoshop software.

Flow cytometric analysis

Bone marrow cells obtained from femora were layered onto a Lympholyte-M gradient (Cedarlane Laboratories Ltd.). After centrifugation, mononuclear cells were collected and stained with anti-RANK (LOB14-8) antibody (Genetex, Inc.) and anti–c-Fms antibody. After two washes, cells were incubated with phycoerythrin-conjugated anti–rat IgG and FITC-conjugated anti–rabbit IgG (Beckman Coulter). Collected mononuclear cells were also fixed, permeabilized, and incubated with phycoerythrin-conjugated anti-CD11b antibody (M1/70; Beckman Coulter) plus FITC-conjugated anti–MOMA-2 antibody (Beckman Coulter). Stained cells were analyzed by Cytomics FC 500 (Beckman Coulter). Simultaneously, mononuclear cells in femurs and tibiae were counted using Flow-Count Fluorospheres (Beckman Coulter).

Measurements of serum TRAP5b activity and calcium

The serum TRAP5b activity was measured using a mouse TRAP assay kit (SBA Sciences). Serum calcium concentrations were measured using a calcium E kit (Wako Chemicals USA, Inc.).

Isolation of c-Fms^+/$RANK^+$ cells and $MOMA\text{-}2^+$/$CD11b^+$ cells

Mononuclear cells obtained from femoral bone marrow were magnetically labeled with biotinylated anti-RANK antibodies conjugated to microbeads using a multiparameter magnetic cell-sorting Antibiotin Multisort kit (Miltenyi Biotec). $RANK^+$ cells were purified using a positive selection column and a Multisort release reagent (Miltenyi Biotec). $RANK^+$ cells were subsequently labeled with anti–c-Fms antibodies conjugated to microbeads using anti–rabbit IgG microbeads (Miltenyi Biotec). c-Fms^+/$RANK^+$ cells were purified using a positive selection column and a Multisort release reagent. $MOMA\text{-}2^+$/$CD11b^+$ cells were similarly purified from femoral bone marrow. Isolated c-Fms^+/$RANK^+$ and $MOMA\text{-}2^+$/$CD11b^+$ cells were cultured for 7 d with 10^4 U/ml M-CSF and 100 ng/ml RANKL with or without 70 µM HU in 96-well plates (1.5 × 10^4 cells).

Statistical analysis

StatView software (version 5.0; SAS Institute, Inc.) was used for all statistical analyses. Data were evaluated by a one-way analysis of variance followed by Fisher's protected least significant difference test. The results of all experiments were expressed as the mean ± SD for 3–8 cultures. $P < 0.05$ was considered statistically significant. Each experiment was repeated at least three times, and similar results were obtained.

Online supplemental material

Fig. S1 shows the expression of cell cycle regulatory molecules in BMMΦ and purified osteoclasts. Fig. S2 shows the effects of overexpression of cell cycle regulatory molecules in BMMΦ on osteoclastogenesis and effects of overexpression of RANK in osteoblasts on cell proliferation. Fig. S3 shows the effects of feeding mice a low calcium diet on the incorporation of BrdU into nuclei of osteoclasts. Fig. S4 shows the characterization of c-Fms^+/$RANK^+$ cells isolated from mouse bone marrow cells. Fig. S5 shows the analysis of QuOPs in c-$Fos^{-/-}$ mice. Online supplemental material is available at http://www.jcb.org/cgi/content/full/jcb.200806139/DC1.

This work was supported in part by Grants-in-Aid (17390497 and 18791376) from the Ministry of Education, Culture, Sports, Science and Technology of Japan. J.M. Penninger is supported by the Austrian Academy of Sciences, the Federal Ministry of Science, and a European Union Excellence Grant.

Submitted: 23 June 2008
Accepted: 23 January 2009

References

Akatsu, T., T. Tamura, N. Takahashi, N. Udagawa, S. Tanaka, T. Sasaki, A. Yamaguchi, N. Nagata, and T. Suda. 1992. Preparation and characterization of a mouse osteoclast-like multinucleated cell population. *J. Bone Miner. Res.* 7:1297–1306.

Arai, F., A. Hirao, M. Ohmura, H. Sato, S. Matsuoka, K. Takubo, K. Ito, G.Y. Koh, and T. Suda. 2004. Tie2/angiopoietin-1 signaling regulates hematopoietic stem cell quiescence in the bone marrow niche. *Cell.* 118:149–161.

Arron, J.R., and Y. Choi. 2000. Bone versus immune system. *Nature.* 408:535–536.

Boyle, W.J., W.S. Simonet, and D.L. Lacey. 2003. Osteoclast differentiation and activation. *Nature.* 423:337–342.

Bucay, N., I. Sarosi, C.R. Dunstan, S. Morony, J. Tarpley, C. Capparelli, S. Scully, H.L. Tan, W. Xu, D.L. Lacey, et al. 1998. osteoprotegerin-deficient mice develop early onset osteoporosis and arterial calcification. *Genes Dev.* 12:1260–1268.

Calvi, L.M., G.B. Adams, K.W. Weibrecht, J.M. Weber, D.P. Olson, M.C. Knight, R.P. Martin, E. Schipani, P. Divieti, F.R. Bringhurst, et al. 2003. Osteoblastic cells regulate the haematopoietic stem cell niche. *Nature.* 425:841–846.

Chambers, T.J. 2000. Regulation of the differentiation and function of osteoclasts. *J. Pathol.* 192:4–13.

Classon, M., and E. Harlow. 2002. The retinoblastoma tumour suppressor in development and cancer. *Nat. Rev. Cancer.* 2:910–917.

Felix, R., M.G. Cecchini, and H. Fleisch. 1990. Macrophage colony stimulating factor restores in vivo bone resorption in the op/op osteopetrotic mouse. *Endocrinology.* 127:2592–2594.

Fischman, D.A., and E.D. Hay. 1962. Origin of osteoclasts from mononuclear leucocytes in regenerating newt limbs. *Anat. Rec.* 143:329–337.

Gerdes, J., H. Lemke, H. Baisch, H.H. Wacker, U. Schwab, and H. Stein. 1984. Cell cycle analysis of a cell proliferation-associated human nuclear antigen defined by the monoclonal antibody Ki-67. *J. Immunol.* 133:1710–1715.

Grigoriadis, A.E., Z.Q. Wang, M.G. Cecchini, W. Hofstetter, R. Felix, H.A. Fleisch, and E.F. Wagner. 1994. c-Fos: a key regulator of osteoclast-macrophage lineage determination and bone remodeling. *Science.* 266:443–448.

Heissig, B., K. Hattori, S. Dias, M. Friedrich, B. Ferris, N.R. Hackett, R.G. Crystal, P. Besmer, D. Lyden, M.A. Moore, et al. 2002. Recruitment of stem and progenitor cells from the bone marrow niche requires MMP-9 mediated release of kit-ligand. *Cell.* 109:625–637.

Hofbauer, L.C., S. Khosla, C.R. Dunstan, D.L. Lacey, W.J. Boyle, and B.L. Riggs. 2000. The roles of osteoprotegerin and osteoprotegerin ligand in the paracrine regulation of bone resorption. *J. Bone Miner. Res.* 15:2–12.

Kawamoto, T., and M. Shimizu. 2000. A method for preparing 2- to 50-micron-thick fresh-frozen sections of large samples and undecalcified hard tissues. *Histochem. Cell Biol.* 113:331–339.

Kim, N., M. Takami, J. Rho, R. Josien, and Y. Choi. 2002. A novel member of the leukocyte receptor complex regulates osteoclast differentiation. *J. Exp. Med.* 195:201–209.

Kodama, H., A. Yamasaki, M. Nose, S. Niida, Y. Ohgame, M. Abe, M. Kumegawa, and T. Suda. 1991. Congenital osteoclast deficiency in osteopetrotic (op/op) mice is cured by injections of macrophage colony-stimulating factor. *J. Exp. Med.* 173:269–272.

Kodama, H., A. Yamasaki, M. Abe, S. Niida, Y. Hakeda, and H. Kawashima. 1993. Transient recruitment of osteoclasts and expression of their function in osteopetrotic (op/op) mice by single injection of macrophage colony-stimulating factor. *J. Bone Miner. Res.* 8:45–50.

Koga, T., M. Inui, K. Inoue, S. Kim, A. Suematsu, E. Kobayashi, T. Iwata, H. Ohnishi, T. Matozaki, T. Kodama, et al. 2004. Costimulatory signals mediated by the ITAM motif cooperate with RANKL for bone homeostasis. *Nature.* 428:758–763.

Kong, Y.Y., H. Yoshida, I. Sarosi, H.L. Tan, E. Timms, C. Capparelli, S. Morony, A.J. Oliveira-dos-Santos, G. Van, A. Itie, et al. 1999. OPGL is a key regulator of osteoclastogenesis, lymphocyte development and lymph-node organogenesis. *Nature.* 397:315–323.

Martin, T.J., E. Romas, and M.T. Gillespie. 1998. Interleukins in the control of osteoclast differentiation. *Crit. Rev. Eukaryot. Gene Expr.* 8:107–123.

Miyamoto, T., F. Arai, O. Ohneda, K. Takagi, D.M. Anderson, and T. Suda. 2000. An adherent condition is required for formation of multinuclear osteoclasts in the presence of macrophage colony-stimulating factor and receptor activator of nuclear factor kappa B ligand. *Blood.* 96:4335–4343.

Mizuno, A., N. Amizuka, K. Irie, A. Murakami, N. Fujise, T. Kanno, Y. Sato, N. Nakagawa, H. Yasuda, S. Mochizuki, et al. 1998. Severe osteoporosis in mice lacking osteoclastogenesis inhibitory factor/osteoprotegerin. *Biochem. Biophys. Res. Commun.* 247:610–615.

Morgan, D.O. 1995. Principles of CDK regulation. *Nature.* 374:131–134.

Morgan, D.O. 1997. Cyclin-dependent kinases: engines, clocks, and microprocessors. *Annu. Rev. Cell Dev. Biol.* 13:261–291.

Naito, M. 1993. Macrophage heterogeneity in development and differentiation. *Arch. Histol. Cytol.* 56:331–351.

Nakayama, K. 1998. Cip/Kip cyclin-dependent kinase inhibitors: brakes of the cell cycle engine during development. *Bioessays.* 20:1020–1029.

Oda, K., Y. Amaya, M. Fukushi-Irie, Y. Kinameri, K. Ohsuye, I. Kubota, S. Fujimura, and J. Kobayashi. 1999. A general method for rapid purification of soluble versions of glycosylphosphatidylinositol-anchored proteins expressed in insect cells: an application for human tissue-nonspecific alkaline phosphatase. *J. Biochem.* 126:694–699.

Okahashi, N., Y. Murase, T. Koseki, T. Sato, K. Yamato, and T. Nishihara. 2001. Osteoclast differentiation is associated with transient upregulation of cyclin-dependent kinase inhibitors p21(WAF1/CIP1) and p27(KIP1). *J. Cell. Biochem.* 80:339–345.

Pavletich, N.P. 1999. Mechanisms of cyclin-dependent kinase regulation: structures of Cdks, their cyclin activators, and Cip and INK4 inhibitors. *J. Mol. Biol.* 287:821–828.

Riggs, B.L., and A.M. Parfitt. 2005. Drugs used to treat osteoporosis: the critical need for a uniform nomenclature based on their action on bone remodeling. *J. Bone Miner. Res.* 20:177–184.

Roodman, G.D. 1999. Cell biology of the osteoclast. *Exp. Hematol.* 27:1229–1241.

Sankar, U., K. Patel, T.J. Rosol, and M.C. Ostrowski. 2004. RANKL coordinates cell cycle withdrawal and differentiation in osteoclasts through the cyclin-dependent kinase inhibitors p27KIP1 and p21CIP1. *J. Bone Miner. Res.* 19:1339–1348.

Sherr, C.J. 1996. Cancer cell cycles. *Science.* 274:1672–1677.

Sherr, C.J., and J.M. Roberts. 1995. Inhibitors of mammalian G1 cyclin-dependent kinases. *Genes Dev.* 9:1149–1163.

Sherr, C.J., and J.M. Roberts. 1999. CDK inhibitors: positive and negative regulators of G1-phase progression. *Genes Dev.* 13:1501–1512.

Suda, T., N. Takahashi, N. Udagawa, E. Jimi, M.T. Gillespie, and T.J. Martin. 1999. Modulation of osteoclast differentiation and function by the new members of the tumor necrosis factor receptor and ligand families. *Endocr. Rev.* 20:345–357.

Takahashi, N., T. Akatsu, N. Udagawa, T. Sasaki, A. Yamaguchi, J.M. Moseley, T.J. Martin, and T. Suda. 1988. Osteoblastic cells are involved in osteoclast formation. *Endocrinology.* 123:2600–2602.

Takahashi, N., N. Udagawa, S. Tanaka, H. Murakami, I. Owan, T. Tamura, and T. Suda. 1994. Postmitotic osteoclast precursors are mononuclear cells which express macrophage-associated phenotypes. *Dev. Biol.* 163:212–221.

Takahashi, N., N. Udagawa, M. Takami, and T. Suda. 2002. Cells of bone: osteoclast generation. *In* Principles of Bone Biology. Second Edition. J.P. Bilezikian, L.G. Raisz, and G.A. Rodan, editors. Academic Press, San Diego, CA. 109–126.

Tanaka, S., N. Takahashi, N. Udagawa, T. Tamura, T. Akatsu, E.R. Stanley, T. Kurokawa, and T. Suda. 1993. Macrophage colony-stimulating factor is indispensable for both proliferation and differentiation of osteoclast progenitors. *J. Clin. Invest.* 91:257–263.

Wang, Z.Q., C. Ovitt, A.E. Grigoriadis, U. Mohle-Steinlein, U. Ruther, and E.F. Wagner. 1992. Bone and haematopoietic defects in mice lacking c-fos. *Nature.* 360:741–745.

Weinberg, R.A. 1995. The retinoblastoma protein and cell cycle control. *Cell.* 81:323–330.

Wiktor-Jedrzejczak, W., and S. Gordon. 1996. Cytokine regulation of the macrophage (M phi) system studied using the colony stimulating factor-1-deficient op/op mouse. *Physiol. Rev.* 76:927–947.

Wiktor-Jedrzejczak, W., A. Bartocci, A.W. Ferrante Jr., A. Ahmed-Ansari, K.W. Sell, J.W. Pollard, and E.R. Stanley. 1990. Total absence of colony-stimulating factor 1 in the macrophage-deficient osteopetrotic (op/op) mouse. *Proc. Natl. Acad. Sci. USA.* 87:4828–4832.

Wilson, A., and A. Trumpp. 2006. Bone-marrow haematopoietic-stem-cell niches. *Nat. Rev. Immunol.* 6:93–106.

Yamamoto, H., N.K. Shevde, A. Warrier, L.A. Plum, H.F. DeLuca, and J.W. Pike. 2003. 2-Methylene-19-nor-(20S)-1,25-dihydroxyvitamin D3 potently stimulates gene-specific DNA binding of the vitamin D receptor in osteoblasts. *J. Biol. Chem.* 278:31756–31765.

Yamamoto, Y., N. Udagawa, S. Matsuura, Y. Nakamichi, H. Horiuchi, A. Hosoya, M. Nakamura, H. Ozawa, K. Takaoka, J.M. Penninger, et al. 2006. Osteoblasts provide a suitable microenvironment for the action of receptor activator of nuclear factor-kappaB ligand. *Endocrinology.* 147:3366–3374.

Yao, Z., P. Li, Q. Zhang, E.M. Schwarz, P. Keng, A. Arbini, B.F. Boyce, and L. Xing. 2006. Tumor necrosis factor-alpha increases circulating osteoclast precursor numbers by promoting their proliferation and differentiation in the bone marrow through up-regulation of c-Fms expression. *J. Biol. Chem.* 281:11846–11855.

Yoshida, H., S. Hayashi, T. Kunisada, M. Ogawa, S. Nishikawa, H. Okamura, T. Sudo, and L.D. Shultz. 1990. The murine mutation osteopetrosis is in the coding region of the macrophage colony stimulating factor gene. *Nature.* 345:442–444.

Zhang, J., C. Niu, L. Ye, H. Huang, X. He, W.G. Tong, J. Ross, J. Haug, T. Johnson, J.Q. Feng, et al. 2003. Identification of the haematopoietic stem cell niche and control of the niche size. *Nature.* 425:836–841.